

AguaClara Cornell Floc Modeling

Fall 2025: Mid-Semester Report

Alex Gardocki (rag325), Lauren Hsu (lkh58), Sarvesh Prabhu (sp2572)

October 17, 2025

Abstract

The Floc Modeling subteam aims to further our understanding of the mechanics of floc formation and clarification in order to improve performance in AguaClara plants through the development of a mathematical model of these processes. This semester, our team is focusing on evaluating the distribution of flocs within the clarifier to test the assumptions of the floc filter clarification model. To analyze the distribution of flocs experimentally, we are employing dye tracers to track the formation and movement of flocs within the floc filter. This will provide evidence to support or refute the assumption that floc saturation is distributed uniformly throughout the floc filter. By combining these experimental results with ongoing efforts to verify our existing models via simulation, we can gain further confidence in our understanding of the mechanisms underlying flocculation and clarification.

Introduction

Flocculation and clarification are critical to the AguaClara treatment process as they remove most primary particles before filtration and chlorination. While these processes are widely used throughout the water treatment industry, gaps remain in our understanding of their underlying physical mechanisms. This lack of understanding has made it challenging to optimize the design of treatment plants and develop automated systems that can successfully respond to fluctuating conditions. It has also prevented the widespread adoption of the novel floc filter technology used in AguaClara plants during clarification. For these reasons, an accurate mathematical model of these processes is essential.

This semester, the Floc Modeling subteam is focusing its efforts on refining the AguaClara clarification model. Clarification is the process following flocculation in which flocs are separated from treated water through settling, also known as sedimentation. During conventional clarification, sedimentation is the sole mechanism for particle removal. However, AguaClara plants utilize an additional process called floc sweeping. Floc sweeping allows previously formed flocs to capture additional primary particles that would settle too slowly on their own, increasing the overall efficiency of clarification. In order to achieve this, vertical jets of water are used to maintain a suspension of flocs known as the floc filter. Primary particles travel up through this suspension, colliding and aggregating with the suspended flocs, which can then be removed. Smaller flocs travel up towards a set of plate settlers, which aggregate these small flocs into larger ones that eventually settle back into the floc filter.

Floc sweeping efficiency depends on coagulant dose, floc filter concentration, and floc saturation. Flocs are initially very porous; as a floc captures primary particles, its pores fill. Eventually, a floc cannot capture any additional particles. Floc saturation is a measurement characterizing how “full” a floc is and how many more particles it is able to capture. Spatial variations in floc saturation within the clarifier can affect particle removal efficiency in the clarifier. If a mathematical model can predict the spatial distribution of flocs in the clarifier, then the areas of the clarifier with the most saturated flocs can be targeted first during wasting. Thus, only flocs that are still capable of capturing primary particles will remain in the clarifier, increasing clarification efficiency.

This semester, the Floc Modeling subteam is investigating the physical properties and interactions between flocs and primary particles in the floc filter during clarification through the use of a lab-scale model vertical clarifier. This model clarifier allows for observation of the floc filter in order to monitor spatial variations in floc filter concentration and floc saturation as well as effluent turbidity under different coagulant dosages and influent conditions. The compact size of the clarifier leads to a low hydraulic residence time, allowing for rapid experimentation and iteration.

Building off the work of the Summer 2025 team, the current subteam is exploring an alternative experimental approach. Rather than tracking floc saturation directly, it relies upon tracking the movement of tracer flocs within the floc filter. This will allow the team to analyze the distribution of flocs within the floc filter and to determine whether or not the floc filter is well-mixed. The results of these experiments can then be applied to validate the assumption of uniform floc saturation within the floc filter.

Literature Review & Previous Work

Previous Work

The Spring 2025 team developed the clarifier shown in Figure 1, and it successfully demonstrated the ability to form a floc filter.

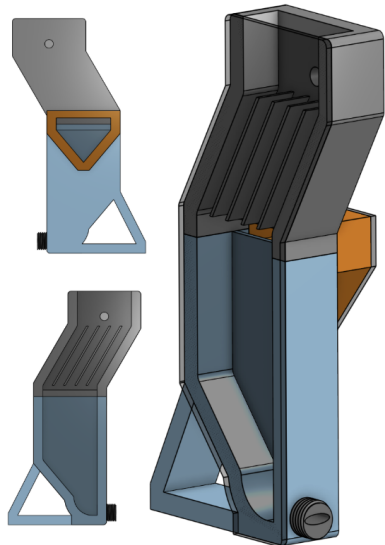


Figure 1. Schematic of prototype model clarifier.

Unfortunately, the grey resin back of the Spring 2025 clarifier made it difficult to distinguish color variations within the clarifier. This was particularly problematic when attempting to analyze the distribution of floc saturation within the floc filter as the proposed method for measuring floc saturation relied upon using colored primary particles to incite a color difference in more saturated regions. The opaque back also prevented the floc filter from being backlit. According to Hurst et al. (2014b), backlighting the floc filter would allow the spatial distribution of floc concentration to be measured via image capture.

For these reasons, the Summer 2025 team redesigned and fabricated a new clarifier, shown in Figure 2, to improve upon the Spring 2025 version. Major changes included utilizing an acrylic plate for both the front and back of the clarifier and adding sampling ports at different heights within the floc filter for taking samples or targeting the removal of saturated flocs. Additional minor adjustments were made to the size and shape of the jet profile, floc weir, and other components.

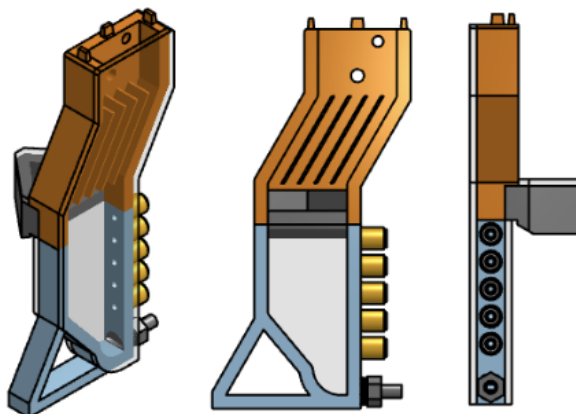


Figure 2. Schematic of revised model clarifier fabricated by the Summer 2025 team.

The Summer 2025 team used this revised model clarifier to test a procedure for measuring floc saturation inspired by Hurst et al. (2014b). First, a floc filter was formed in the clarifier by running white kaolin clay and poly-aluminum chloride (PACl) coagulant through a tube flocculator to make uncolored flocs. Then, colored clay primary particles were added to the clarifier directly. The expectation was that these colored particles would be captured by the flocs within the floc filter, leading to a color change in the more saturated regions of the clarifier. A diagram of the experimental apparatus used is pictured in Figure 3. Following the addition of colored clay, pictures of the floc filter were taken for further analysis.

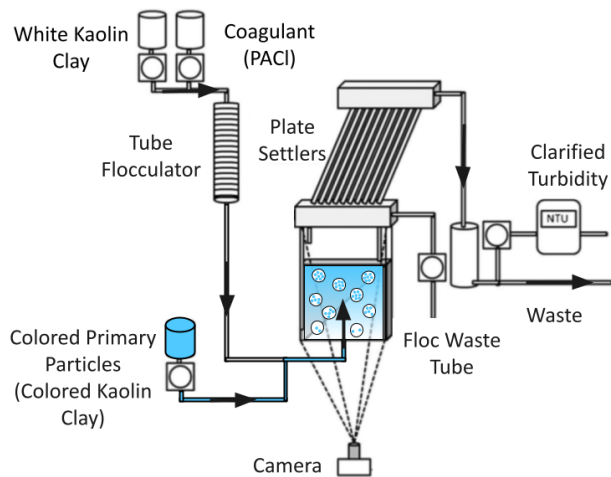


Figure 3. A diagram of the proposed experimental apparatus for detecting variations in floc saturation within the floc filter. Adapted from Hurst et al., 2014a.

Each floc filter image was processed in ImageJ by separating red, green, and blue channels, cropping to the filter region, and calculating average pixel brightness by row to assess how brightness changed with height. Unfortunately, it appeared that variations in lighting intensity influenced results far more than coloration differences, and no direct connection could be drawn between floc saturation and color intensity. Thus, the effectiveness of the floc filter imaging method remained unclear. This prompted the adoption of the new experimental procedure being used this semester.

Floc Bond Strength

This semester we conducted a literature review through the review paper of Jarvis et al. (2005), which provides a foundational framework for understanding floc formation and breakage dynamics in water treatment systems. According to Jarvis et al., floc growth reaches equilibrium when aggregation and breakage forces balance, mathematically expressed as the collision rate multiplied by efficiency minus the breakage rate. Two key mechanisms of breakage are highlighted: surface erosion, where tangential shear stress removes particles from floc surfaces, and large scale fragmentation, where tensile stress splits flocs into similar sized pieces. The

review categorizes measurement techniques into macroscopic and microscopic approaches. Macroscopic methods include the floc strength factor, which quantifies the ratio of floc size before and after shear exposure, and shear based models that link floc size to applied velocity gradients. Microscopic methods, on the other hand, involve micromechanical tests that measure tensile rupture forces and micromanipulation techniques that compress flocs, though the latter has limited operational relevance.

A consistent theme across studies is that smaller flocs are inherently stronger than larger ones. This is attributed to increased compaction, higher bond density per unit volume, and the selective removal of weaker bonds during breakage, which leaves behind stronger remnants. Coagulation chemistry also plays a critical role in floc stability. Optimum coagulant dosing produces maximum floc strength, but this does not increase linearly with dose; instead, strength peaks and then declines at intermediate concentrations before recovering at higher levels, as described by Francois (1987) and Bache et al. (1999). Furthermore, bridging mechanisms such as sweep flocculation tend to yield stronger flocs than charge neutralization, while polymer additions show mixed outcomes, enhancing strength in chemical flocs but reducing stability in biological systems.

Recent comparisons, such as those by Yukselen and Gregory (2004), reveal that hydrolyzing coagulants like alum and polyaluminium chloride produce weaker flocs than cationic polyelectrolytes, challenging the assumption that metal coagulants are always the most effective. Jarvis et al. further argue that perfect charge neutralization may actually weaken flocs by causing particles to stick at first contact rather than reorganize into stronger structures. Instead, slight under or overdosing may enhance resilience by maintaining controlled repulsion, which allows for structural optimization. This perspective suggests that current coagulation practices may be optimized for aggregation efficiency rather than long term floc strength, offering an explanation for why many treatment plants achieve good initial removal yet still encounter floc breakage problems. More recent studies, particularly those examining interactions between polyaluminium chloride and humic acids, extend this discussion but remain underexplored, pointing to an important direction for future research.

Dye Selection

The dye Red-40 was evaluated for its potential usage in flocculation/clarification experiments. Red-40 is an anionic azo dye with sulfonate groups that impart a negative charge in aqueous solutions; it has chemical formula C₁₈H₁₄N₂Na₂O₈S₂ and molecular weight 496.4 g·mol⁻¹.

Existing literature focused on adsorption of Red-40 onto chitosan. According to Kumar et al. (2000), chitosan is a cationic polysaccharide that is made from chitin deacetylation; chitin is found in insect exoskeletons, crustaceans shells, and fungal cell walls. Pinto et al. (2009) demonstrated that the protonated amino group in chitosan yields a positive charge, facilitating strong electrostatic interactions with the negatively charged sulfonate groups on Red-40 and leading to strong adsorption between chitosan and Red-40.

Pinto et al. (2011) demonstrated the Red-40 adsorption onto chitosan follows pseudo-second-order and Elovich kinetic models, suggesting that the adsorption occurs through chemical interactions in addition to physical interactions. Infrared spectroscopy results showed evidence of the electrostatic interaction between the amine group of chitosan and the sulfonated group of Red-40. Furthermore, thermodynamic data from Pinto et al. (2009) indicate the adsorption of Red-40 on chitosan is an exothermically-controlled process. These findings indicate that Red-40 adsorption onto chitosan is favorable.

PACl Coagulant and chitosan shared key characteristics that showed promise for Red-40 adsorption onto coagulant. Both chitosan and coagulant have a net positive surface charge under acidic to near-neutral pH, favoring adsorption of anionic dyes such as Red-40. The aluminum hydroxide complexes in coagulant can act in a manner similar to protonated amine groups in chitosan, interacting with Red-40's sulfonated group. Thus, the use of Red-40 as a dye for the floc filter showed promise.

Clarification Modeling

Vitasovic (1986) and Takacs et al. (1991) developed a 1D model of clarification based on solids flux theory to predict the sludge blanket settling velocity. The Takacs model unified the description of both discrete and hindered settling into a single equation. However, Gernaey et al. (2001) highlighted the difficulty of fitting this model, limiting its utility in practical applications. Head et al. (1997) modeled floc blanket clarification by examining how influent concentration and floc wastage flow rate influence the height and concentration of the floc blanket. However, the model is limited in its ability to describe how particle size distribution post-flocculation and coagulant dosage impact clarification performance.

Sarmiento (2021) addressed this gap by applying the Pennock et al. (2018) flocculation model which accounts for coagulant dosage and distinguishes between the settleable and non-settleable particles formed during flocculation. Sarmiento (2021) assumes that all settleable particles generated during flocculation are removed during clarification. In contrast to model predictions, experimental results indicate that clarification performance decreases over time, possibly due to effects of floc saturation. Pennock et al. (2023) modified the Pennock et al. (2018) flocculation model to describe how the conversion from non-settleable to settleable particles depends on clarifier design. Nonetheless, their work did not incorporate floc sweeping and floc saturation, which are of significance in floc filter-based clarifiers. In the summer of 2024, our team built on these models to account for floc sweeping and floc saturation. Despite these enhancements, discrepancies between experimental and theoretical parameter values exist, indicating the need to reevaluate the assumptions of the model. The major assumptions are that flocs in the floc filter are at their steady-state saturation level and the floc filter is well-mixed. Therefore experimentation is needed to investigate the spatial and temporal dynamics of the floc filter. This semester, the subteam will look into whether floc movement probabilities between positions remain constant across time steps ie. testing if flocs move independently rather than collectively in discrete layers.

Methods

Experimental Apparatus

For our experiments, we used a tube flocculator paired with the low hydraulic residence time model clarifier developed by the Summer 2025 team. The tube flocculator had a radius of curvature of 42 mm and an inner diameter of 4.381 mm. Based on calculations described by Tse et al. (2011), at a flow rate of 1.2 mL/s, this gave a velocity gradient of $G = 145 \text{ Hz}$. This flow rate also gave a hydraulic residence time of $\theta = 304 \text{ seconds}$.

The parameters of the clarifier were chosen to mimic the characteristics of an actual AguaClara clarifier. The cross-sectional area of the clarifier was designed to be 1200 mm^2 in order to achieve an upflow velocity of 1 mm/s given a flow rate of 1.2 mL/s since this is the upflow velocity used in AguaClara plants (Weber-Shirk, n.d.). The average initial velocity at the jet was 17 mm/s based on the cross-sectional area of the jet inlet, which was 71 mm^2 . This larger initial velocity ensured the jet would have sufficient momentum to keep the floc filter suspended.

For the plate settlers, a spacing of 1 cm between plates was chosen to avoid floc rollup. Using the equation found in the AguaClara textbook (Weber-Shirk, n.d.), we calculated the necessary plate settler length to be 14.67 cm to ensure the AguaClara standard capture velocity of 0.12 mm/s. However, due to limitations in print size, we chose to reduce the length to 7.33 cm, resulting in a capture velocity of 0.21 mm/s. A plate width of 2.0 mm was chosen to balance the integrity of the print with having the thinnest plates possible to reduce the increase in upflow velocity through the plate settlers. The plates were placed at a 60° angle based on AguaClara clarifier specifications (Weber-Shirk, n.d.). The area above the plate settlers was left open to the air to prevent air bubbles from being trapped in a closed system.

During operation, coagulant and a turbidity source (typically white kaolin clay) were first added to the influent of the tube flocculator. After exiting the flocculator, the newly formed flocs were directed into the clarifier. The jet reverse maintained these flocs in suspension in order to form a floc filter within the clarifier. Excess flocs were removed via a floc hopper, which drained flocs from the floc filter once they reached a height of 124 mm above the diffuser.

Experimental Design

Our proposed method for tracking the movement of flocs within the floc filter is as follows. First, a colorless floc filter will be formed from white kaolin clay and poly-aluminum chloride (PACl) coagulant. Next, a small number of colored flocs will be formed by combining Red-40, white kaolin clay, and PACl. The white kaolin clay will still make up the majority of the contents of the flocs so that their properties are comparable to the uncolored flocs. These colored flocs will then be inserted into the clarifier, allowing us to track the movement of these tracer flocs within the floc filter. Figure 4 shows a process flow diagram of this full process. From this, we can determine if the motion of flocs within the floc filter is independent of their current location or if the flocs tend to move in discrete sections. If the movement is random and the

colored flocs quickly become uniformly distributed within the floc filter, then it follows that floc saturation will also be uniformly distributed within the clarifier.

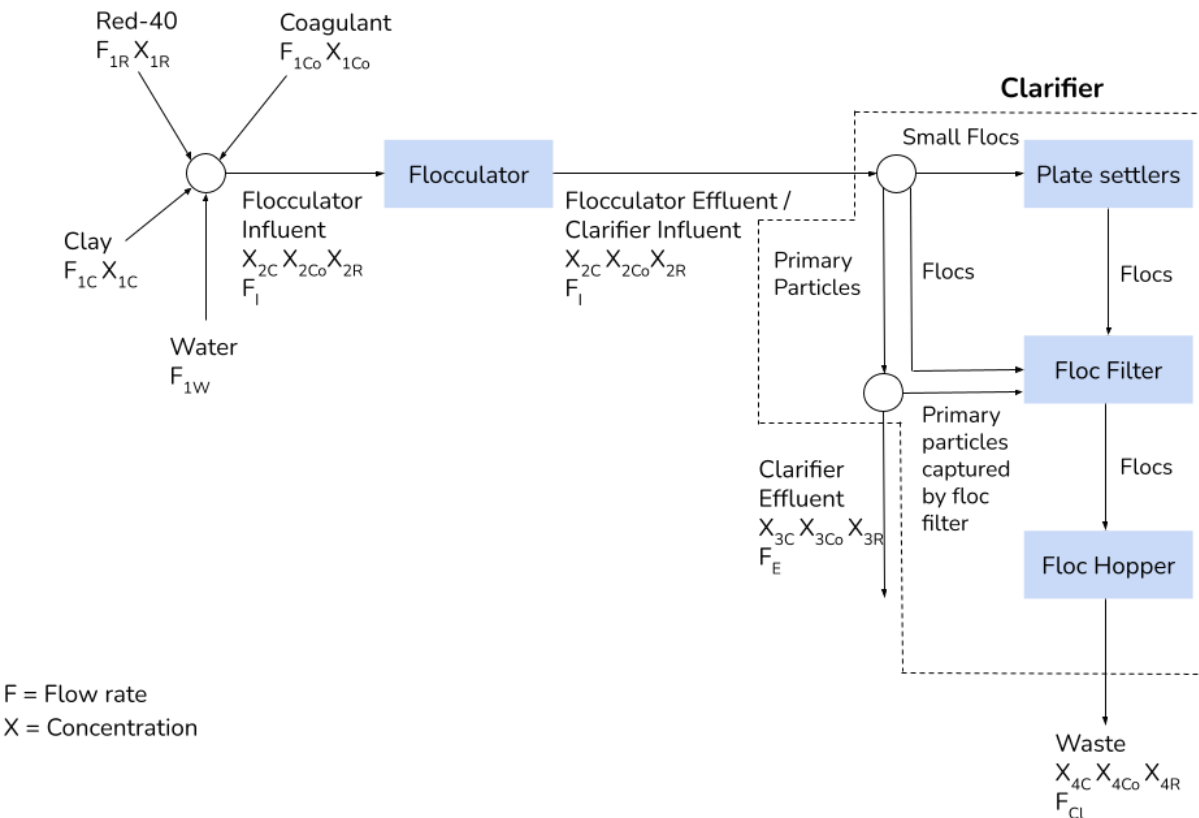


Figure 4. Process flow diagram illustrating movement of clay, coagulant, and Red-40 through the experimental setup.

In order to ensure that this procedure would work, we first had to verify that we could make colored flocs using Red-40. We tested this in two phases. First, we attempted to form colored flocs using only Red-40 and PACl . A solution of 40 mg/L of Red-40 and 10 mg/L of PACl was added to the flocculator over the course of 80 minutes, providing ample time for floc filter formation. Due to an oversight when initializing the ProCoDA method file, a flow rate of 1.3 mL/s was used rather than the typical 1.2 mL/s. After 20 minutes had elapsed, the concentration of PACl was increased to 20 mg/L to promote larger floc formation.

In the second phase, we attempted to form flocs containing both kaolin clay and Red-40. Over the course of 15 minutes, a solution of 46 mg/L of white kaolin clay, 4 mg/L of Red-40, and 20 mg/L of PACl was added to the flocculator. After testing for the formation of colored flocs, we continued building the floc filter using a solution of 50 mg/L of white kaolin clay and 20 mg/L of PACl in order to test if the colored flocs could be distinguished from uncolored flocs.

After these initial tests, we tried implementing our procedure for tracking the movement of flocs in the floc filter. A solution of 50 mg/L of white kaolin clay and 20 mg/L of PACl was added to the flocculator over the course of 50 minutes in order to form an uncolored floc filter. Afterwards, a solution of 46 mg/L of white kaolin clay, 4 mg/L of Red-40, and 20 mg/L of PACl was added for 10 minutes in order to introduce a small number of colored flocs. Finally, the influent solution was returned to the original 50 mg/L of white kaolin clay and 20 mg/L of PACl in order to monitor the movement of the colored flocs over an additional 20 minutes.

Results

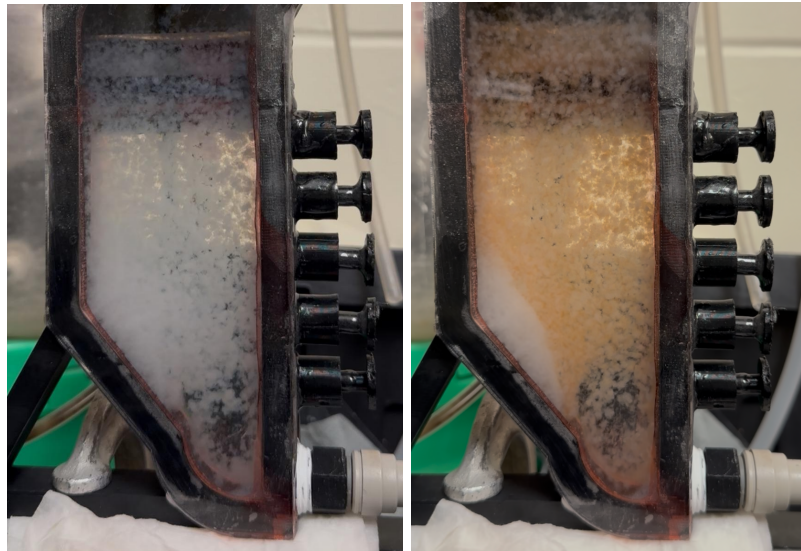
The initial experiment for forming flocs from Red-40 and PACl showed promising results. The Red-40 successfully formed large, healthy flocs to populate the floc filter, as shown in Figure 5. Residual dissolved Red-40 in the clarifier which had not been incorporated into flocs caused the water to be dyed a deep red. Although this made it harder to see the colored flocs, this behavior was expected due to the extremely high concentration of Red-40 being used.



Figure 5. Floc filter formed from Red-40 and PACl.

The flocs formed from Red-40 combined with white kaolin clay were also promising. While the coloration was lighter due to the smaller concentration of Red-40, the flocs were still distinctly red. As a side effect of the lower Red-40 concentration, there was also less residual Red-40 to dye the water, meaning the flocs did not blend in as much with the surrounding water. However, after ceasing the addition of Red-40, the flocs entering the floc filter continued to be red. Even after 25 minutes of adding white kaolin clay flocs without any additional Red-40, the entire floc filter remained the same color, with no discernible differentiation between the colored and uncolored flocs.

The results of the last experiment were similar. We hypothesized that the continued red coloration could have been coming from residual Red-40 that was stuck to the walls of the flocculator, so before starting the experiment, we cleaned the flocculator using distilled vinegar in order to neutralize any PACl which was allowing the Red-40 to adhere to the walls. This seemed to work as the initial uncolored floc filter formed successfully without any red coloration, as seen in Figure 6(a). However, once the Red-40 was added, the coloration quickly spread throughout the entire floc filter as shown in Figure 6(b), with the exception of a small corner of the diffuser where the flocs appeared to be too tightly packed together to admit any dye.



Figures 6(a), 6(b). Floc filter before (a) and after (b) addition of Red-40.

Discussion

Based on the manner in which the coloration spread through the floc filter after the addition of Red-40, it is likely that residual dissolved Red-40 that has not been flocculated is spreading throughout the clarifier and quickly adsorbing onto flocs, leading to the sudden color change observed throughout the floc filter. Unfortunately, due to the potency of Red-40 as a dye and its solubility, it would be extremely difficult if not impossible to remove all Red-40 from solution through flocculation. It is also possible that part of the coloration of the flocs comes from pockets of dyed water within the flocs, in which case the Red-40 would simply diffuse down the concentration gradient and into the undyed flocs. For these reasons, Red-40 may not be a viable choice as a tracer dye within the clarifier.

Future Work

We will continue experimenting with Red-40 to see if a lower concentration of dye may be able to dye flocs within the flocculator without so quickly spreading this coloration into the clarifier. Additionally, we plan to reconsider using different colors of clay as a source for colored

particles. While previous work has shown that capturing colored clay primary particles has little effect on the color of a floc, it has also shown that flocs formed entirely out of colored clay particles tend to exhibit a noticeable coloration in comparison to flocs formed from white kaolin clay. Hence, rather than adding Red-40 in order to induce coloration, we plan to experiment with switching between white kaolin clay and colored kaolin clay in order to create colored flocs. Since the coloration of colored clay particles tends to be stable, this will hopefully prevent any issues with dye diffusing into other flocs within the floc filter.

Appendix

Section I: Mass Balance Calculations for Experimentation

Total influent flow rate (mL/s)	1.2
Effluent flow rate (mL/s)	1.2
Clay/coagulant/Red-40 influent flow rate (mL/s)	x
Clay/coagulant/Red-40 influent concentration (M)	c
Clay/coagulant/Red-40 stock concentration (M)	s
Clay/coagulant/Red-40 pump volume per revolution (mL/rev)	n
Clay/coagulant/Red-40 pump speed (rev/s)	v
Water flow rate (mL/s)	w
Waste flow rate (mL/s)	a
Effluent with wasting flow rate (mL/s)	e

The equations below were used to determine the flow rates and pump speeds during the experiment.

$$x = \frac{1.2 c}{s}$$

$$v = \frac{60 x}{n}$$

$$w = 1.2 - x_{clay} - x_{coag} - x_{red}$$

$$e = 1.2 - a$$

References

- Bache, D. H., Rasool, E., Moffat, D., & McGilligan, F. J. (1999). On the strength and character of Alumino-Humic Flocs. *Water Science and Technology*, 40(9).
[https://doi.org/10.1016/s0273-1223\(99\)00643-5](https://doi.org/10.1016/s0273-1223(99)00643-5)
- François, R. J. (1987). Strength of aluminium hydroxide flocs. *Water Research*, 21(9), 1023–1030. [https://doi.org/10.1016/0043-1354\(87\)90023-6](https://doi.org/10.1016/0043-1354(87)90023-6)
- Gernaey, K., Vanrolleghem, P. A., & Lessard, P. (2001). Modeling of a reactive primary clarifier. *Water Science & Technology*, 43(7), 73–81. <https://doi.org/10.2166/wst.2001.0393>
- Head, R., Hart, J., & Graham, N. (1997). Simulating the effect of blanket characteristics on the floc blanket clarification process. *Water Science & Technology*, 36(4).
[https://doi.org/10.1016/s0273-1223\(97\)00422-8](https://doi.org/10.1016/s0273-1223(97)00422-8)
- Hurst, M., Weber-Shirk, M., Charles, P., & Lion, L. W. (2014a). Apparatus for observation and analysis of Floc Blanket Formation and performance. *Journal of Environmental Engineering*, 140(1), 11–20. [https://doi.org/10.1061/\(asce\)ee.1943-7870.0000773](https://doi.org/10.1061/(asce)ee.1943-7870.0000773)
- Hurst, M., Weber-Shirk, M., & Lion, L. W. (2014b). Image analysis of floc blanket dynamics: Investigation of floc blanket thickening, growth, and steady state. *Journal of Environmental Engineering*, 140(4). [https://doi.org/10.1061/\(asce\)ee.1943-7870.0000817](https://doi.org/10.1061/(asce)ee.1943-7870.0000817)
- Jarvis, P., Jefferson, B., Gregory, J., & Parsons, S. A. (2005). A review of floc strength and breakage. *Water Research*, 39(14), 3121–3137.
<https://doi.org/10.1016/j.watres.2005.05.022>
- Kumar, M. N. V. R. (2000). A review of chitin and chitosan applications. *Reactive and Functional Polymers*, 46(1), 1–27. [https://doi.org/10.1016/S1381-5148\(00\)00038-9\[1\]](https://doi.org/10.1016/S1381-5148(00)00038-9[1])
- Pennock, W. H., Weber-Shirk, M. L., & Lion, L. W. (2018). A hydrodynamic and surface coverage model capable of predicting settled effluent turbidity subsequent to hydraulic flocculation. *Environmental Engineering Science*, 35(12), 1273–1285.
<https://doi.org/10.1089/ees.2017.0332>
- Pennock, W. H., Lion, L. W., & Weber-Shirk, M. L. (2023). Simple model for coupled hydraulic flocculation-sedimentation performance. *Journal of Environmental Engineering*, 149(12). <https://doi.org/10.1061/joeedu.eeeng-7384>
- Piccin, J. S., Dotto, G. L., Vieira, M. L. G., & Pinto, L. A. A. (2009). Adsorption of FD&C Red No. 40 by chitosan: Isotherms analysis. *Chemical Engineering Journal*, 150(2–3), 366–373. <https://doi.org/10.1016/j.jfoodeng.2009.03.017>

Piccin, J. S., Vieira, M. L. G., Dotto, G. L., & Pinto, L. A. A. (2011). Kinetics and mechanism of the food dye FD&C Red 40 adsorption onto chitosan. *Journal of Chemical & Engineering Data*, 56(10), 3759–3765. <https://doi.org/10.1021/je200388s>

Sarmiento, K. (2021). Particle Removal in Floc Blanket Clarifiers Via Internal Flow Through Porous Fractal Aggregates. *Cornell University*.

Takács, I., Patry, G., & Nolasco, D. (1991). A dynamic model of the clarification-thickening process. *Water Research*, 25(10), 1263–1271.
[https://doi.org/10.1016/0043-1354\(91\)90066-y](https://doi.org/10.1016/0043-1354(91)90066-y)

Tse, I. C., Swetland, K., Weber-Shirk, M. L., & Lion, L. W. (2011). Method for quantitative analysis of flocculation performance. *Water Research*, 45(10), 3075–3084.
<https://doi.org/10.1016/j.watres.2011.03.021>

Vitasovic, Z. Z. (1986). An Integrated Control Strategy for the Activated Sludge Process. Rice University.

Weber-Shirk, M. (n.d.). *The Physics Of Water Treatment Design*.
<https://aguaclara.github.io/Textbook/index.html>

Yukselen, M. A., & Gregory, J. (2004). The effect of rapid mixing on the break-up and re-formation of Flocs. *Journal of Chemical Technology & Biotechnology*, 79(7), 782–788. <https://doi.org/10.1002/jctb.1056>